To conclude, we have demonstrated in this paper a new method of estimating rate coefficients, which can be used with highly ionized ions previously not accessible (because of the lower electron temperature in θ pinches). Given the wide variety of central electron temperatures which can be obtained in existing tokamaks (roughly 100 eV $\lesssim T_e \lesssim$ 3 keV), this method should allow ionization and recombination rate coefficients to be estimated for a large number of ions of the same impurity, and for a large number of elements. The precision of this type of estimations (which is already not much worse than in previous work) can be improved by increasing the signal-to-noise ratio of the observed emission, and probably also by using electron-temperature conditions such that the sawtooth modulations exist on the emission of two successive ions. Finally, previous work on θ pinches has also been used to estimate excitation-rate coefficients, by introducing into the discharge known amounts of a given impurity and measuring the intensities absolutely. This technique is, of course, also possible here.

[1]K. T. Dolder, in *Case Studies in Atomic Collision Physics*, edited by E. W. McDaniel and M. R. C. McDowell (North-Holland, Amsterdam, 1969), Vol. 1, p. 250.

[2]H. J. Kunze, Space Sci. Rev. 13, 565 (1972).

[3]S. von Goeler, W. Stodiek, and N. Sauthoff, Phys. Rev. Lett. 33, 1201 (1974).

[4]R. R. Smith, Nucl. Fusion 16, 225 (1976).

[5]J. D. Callen and G. L. Jahns, Phys. Rev. Lett. 38, 491 (1977).

[6]TFR Group, Plasma Phys. 19, 349 (1977).

[7]TFR Group, in *Proceedings of the Sixth International Conference on Plasma Physics and Controlled Ncuelar Fusion Research, Berchtesgaden, 1976* (International Atomic Energy Association, Vienna, 1977), Vol. 1, p. 279.

[8]The exact wavelengths of these two transitions have been shown to be 115.97 and 127.81 Å; see P. G. Burkhalter, J. Reader, and R. D. Cowan, J. Opt. Soc. Am. 67, 1521 (1977); M. W. D. Mansfield, N. J. Peacock, C. C. Smith, M. G. Hobby, and R. D. Cowan, J. Phys. B 11, 1521 (1978).

[9]TFR Group, Plasma Phys. 19, 587 (1977).

[10]C. Breton, C. De Michelis, and M. Mattioli, J. Quant. Spectrosc. Radiat. Transfer 19, 367 (1978).

[11]W. Lotz, Max Planck Institut für Plasma-Physik, Garching, Internal Reports No. IPP 1/62, 1967 and No. IPP 1/76, 1968 (unpublished).

[12]S. Von Goeler, W. Stodiek, H. Eubank, H. Fishman, S. Grebenshchikov, and E. Hinnov, Nucl. Fusion 15, 301 (1975).

[13]A. Burgess, Astrophys. J. 141, 1588 (1965).

Ion-Cyclotron Instability in the TFR Tokamak

TFR Group[a]

Association EURATOM-Commissariat à l'Energie Atomique sur la Fusion, Département de Physique du Plasma et de la Fusion Contrôlée, Centre d'Etudes Nucléaires, 92260 Fontenay-Aux-Roses, France

(Received 24 January 1978)

Density fluctuations in the ion-cyclotron frequency range have been observed in the TFR tokamak by microwave scattering. The geometry was such that the selected fluctuation wave vector was aligned across the confining magnetic field in the outside region of the torus. A threshold for the onset of the instability as a function of the discharge current has been observed. A plausible explanation of this instability in terms of current-driven ion-cyclotron electrostatic wave is discussed.

There is an extensive experimental and theoretical literature on ion-cyclotron instability in low-temperature plasma.[1-4] To our best knowledge there is no experimental observation of this kind of instability in tokamak devices. In this Letter, we present the first experimental evidence of the presence of density fluctuations in the region of the ion-cyclotron frequency and its harmonics in the TFR tokamak.

The electron density fluctuations have been observed by means of a microwave scattering experiment. Figure 1 is a schematic block diagram of the experimental arrangement. A 75-GHz, 10-W wave polarized in the extraordinary mode was launched into the plasma. This mode has been chosen because it permits propagation of the wave beam with negligible refraction for most of the TFR operating conditions. For the

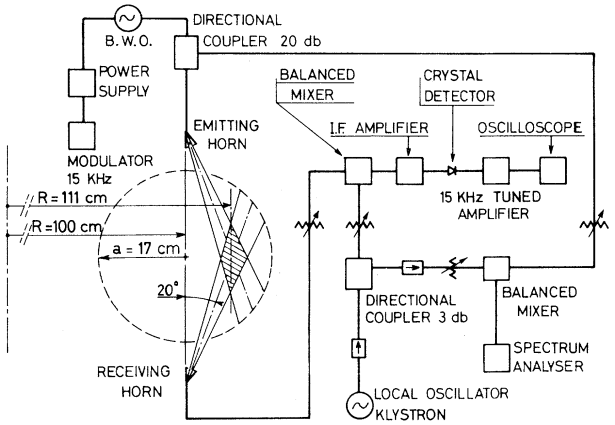

FIG. 1. Schematic diagram of the experimental arrangement.

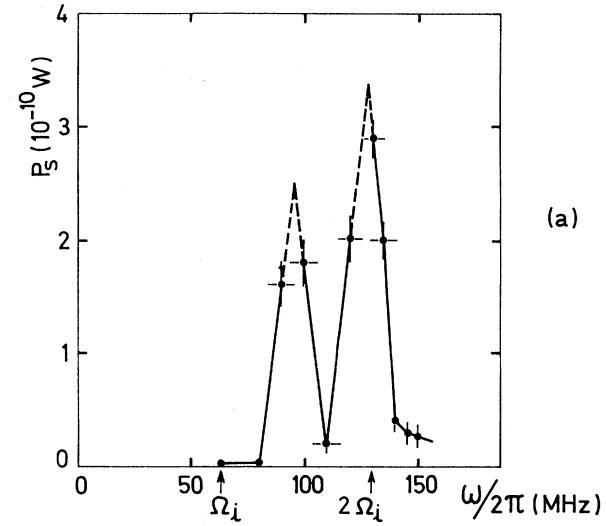

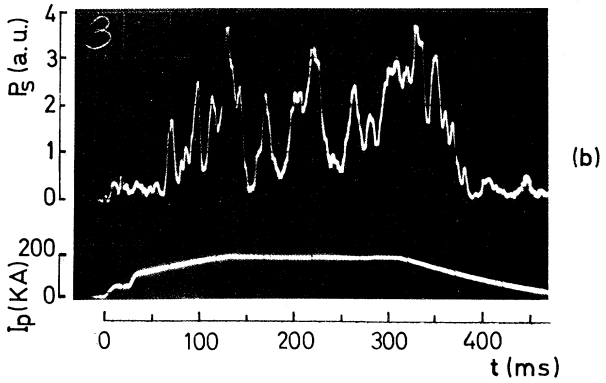

FIG. 2. (a) The scattered power P_s as a function of the frequency $\omega/2\pi$ at t = 280 ms. Hydrogen, $\bar{n}_e(r = 11$ cm) = 1.0×10^{13} cm^{-3}, $T_e(r = 11$ cm) = 800 eV, $T_e(r = 0) = 2.1$ keV, I = 200 kA, B = 49 kG, a = 17 cm, $T_e/T_i(r = 11$ cm) = 2. The arrows indicate the values of Ω_i and $2\Omega_i$ at r = 11 cm, the center of the scattering volume. (b) The scattered power P_s as function of time for $\omega/2\pi$ = 90 MHz corresponding to the first peak of (a) (upper trace) and the discharge current I (lower trace).

extraordinary polarization the accessibility condition is $f_{c0} < f < f_{ce}$, where $f_{c0} = -f_{ce}/2 + [(f_{ce}/2)^2 + f_{pe}^2]^{1/2}$ is the cutoff frequency and f_{ce} and f_{pe} are the electron cyclotron and plasma frequencies, respectively. For a toroidal magnetic field $B_{tor} \geq 30$ kG and the plasma density in the interval $2 \times 10^{13} - 10^{14}$ cm^{-3} we find $f_{c0} = 16-60$ GHz. The incident frequency is selected in the 4-mm wavelength band where cw power sources in the range of 10–100 W are available.

A conventional superheterodyne receiver is used with an intermediate-frequency bandwidth $\Delta f = \pm 5$ MHz followed by a synchronous amplifier tuned to the frequency (15 kHz) of the amplitude modulation of the source in order to avoid the unwanted direct plasma radiation.

The frequency and wave vector $\vec{k}$ of the density fluctuations must satisfy the usual synchronism conditions $\omega = \omega_i - \omega_s$ and $\vec{k} = \vec{k}_i - \vec{k}_s$ where the subscripts i and s stand for the incident and scattered wave, respectively. In our experiment the geometry of the incident and scattered beam is such that the wave vector $k = k_\perp = 2k_i \sin\frac{1}{2}\theta_s = 11$ cm^{-1} ($k_i \approx k_s$) is aligned across the magnetic field with a fixed scattering angle $\theta_s = 40°$.

In Fig. 2(a) we present the scattered power P_s versus $\omega/2\pi$ for the discharge condition noted, at the time t = 280 ms during the plateau of the plasma current. These data were obtained by setting the emitter frequency at 75 GHz, and changing, shot by shot, the frequency of the local oscillator. The frequency resolution was set by the received bandwidth $\Delta f = \pm 5$ MHz, and the spatial resolution $\Delta r \approx 6$ cm resulted from the emitting and receiving horn lobe width.

In Fig. 2(b) the time evolution of P_s is shown for $\omega/2\pi$ = 90 MHz corresponding to the first maximum of the spectrum of Fig. 2(a). For comparison, the discharge current is also presented.

The pattern of the frequency spectrum is very peculiar and shows a first peak close to Ω_i, and a second peak practically at $2\Omega_i$, whereas the time evolution of P_s shows a current threshold for the onset and disappearence of the instability.

We now try to explain the observed peaks as current-driven ion-cyclotron waves. We assume an isotropic Maxwellian velocity distribution for ions and electrons ($T_e \neq T_i$), with an electron drift velocity v_D along the magnetic field. The homogeneous plasma dispersion relation for the

electrostatic ion-cyclotron waves (EICW), propagating at an arbitrary angle, is given by[2-4]

$$\epsilon(\vec{k}, \omega) = 1 + \sum_j \frac{1}{k^2 \lambda_{Dj}^2} \sum_{n=-\infty}^{\infty} \Gamma_j(b_j) A_{nj}, \qquad (1)$$

where $A_{nj} = 1 + \xi_{0j} Z(\xi_{nj})$, $\xi_{nj} = (\omega - k v_{Dj} - n\Omega_j)/\sqrt{2}\, k_\parallel v_j$, Z is the plasma dispersion function, $\lambda_{Dj}^2 = v_j^2/\omega_{pj}^2$, $\omega_{pj}^2 = 4\pi n e^2/m_j$, $v_j = (T_j/m_j)^{1/2}$, $b_j = (k_\perp \rho_j)^2$, $\rho_i = v_j/\Omega_j$, $\Omega_j = eB/m_j c$, and $\Gamma_{nj} = \exp(-b_j) I_n(b_j)$. We now assume $k_\perp > k_\parallel$; and for the parameters of our experiment, $k_i \rho_e \ll 1$, $\Gamma_{0e} = 1$, $\Gamma_{ne} = 0$ for $n \neq 0$, $\xi_{0e} \ll 1$ $(v_D/v_e \ll 1)$, $(\omega - \Omega_i)/k_\parallel v_i > 1$, $v_e > v_D > v_i$. By retaining the nth term only in Eq. (1), for the real part of the dispersion relation we obtain

$$\frac{\omega - n\Omega_i}{n\Omega_i} \approx \frac{T_e}{T_i} \Gamma_n. \qquad (2)$$

From the experimental values of T_e/T_i at $t = 280$ ms (only T_e has been measured simultaneously with the scattering experiment and the ratio T_e/T_i is inferred from similar discharges) and $k_\perp = 11$ cm^{-1}, the value at the center of the scattering volume, from Eq. (2) for $n = 1$ we obtain $(\omega - \Omega_i)/\Omega_i = 0.29$ and for $n = 2$ we obtain $(\omega - 2\Omega_i)/2\Omega_i = 0.03$, to be compared with 0.45 and almost ~0 corresponding to the first and second peaks of Fig. 2(a), respectively.

In Fig. 3 we have plotted $\omega/2\pi$ from Eq. (2) versus time, using the experimental values of T_e/T_i, for three values of the wave vector $k_\perp$ corresponding respectively to the center and to borders of the scattering volume. In this experiment we were not able to make a $k_\perp$ scan and the selected value was $k_\perp = 11 \pm 3$ cm^{-1}, the resolution being set by the antenna lobe widths measured at 3 dB. The experimental points, also shown on Fig. 3, correspond to the first peak of the frequency spectrum measured at different times. These points seem to fit the dispersion relation better at the outside border of the $k_\perp$ interval. Note that if we assume $k_\perp = 14$ cm^{-1}, as suggested by Fig. 3, we obtain $(\omega - \Omega_i)/\Omega_i = 0.36$ which is very close to the experimental value for the first peak. For $n = 2$, $(\omega - 2\Omega_i)/2\Omega_i = 0.08$ which is of the same order of our frequency resolution. In Eq. (1) we have disregarded the effects of the plasma inhomogeneity[5] since in our experiment

$$\Omega_i \gg \omega_{e,i}^* = (k_\theta c T_{e,i}/q_{e,i} B)(1/n)(dn/dx)$$

if we assume $k_\theta \sim k_r \sim 14$ cm^{-1}. In view of the uncertainty of the value of T_e/T_i (50% accuracy), the experimental results seem in good agreement with Eq. (2).

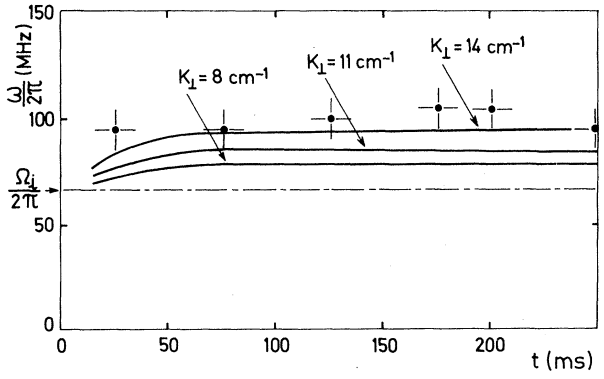

FIG. 3. The frequency $\omega/2\pi$ calculated from Eq. (2) for the experimental conditions of Fig. 2(a) versus time for three values of $k_\perp$ (solid lines). The experimental points correspond to the first maximum of the measured frequency spectra.

We now discuss the possible excitation mechanism of the EICW.

The current-driven instability, which has been very often observed in the low-temperature plasma experiments, is characterized by a growth rate given by[2]

$$\gamma \approx \left(\frac{\pi}{2}\right)^{1/2} n\Omega_i \frac{T_e}{T_i} \Gamma_n \left(\frac{v_D}{v_e} - \frac{n\Omega_i}{k_\parallel v_e}\right). \qquad (3)$$

The maximum growth rate occurs for $k_\perp \rho_i \sim 1$ $(\Gamma_1 = 0.2)$, and the critical drift is given by

$$\frac{v_D}{v_i} \geq \left(\frac{T_i}{\Gamma_1 T_e} + 1\right)\left(\ln \frac{m_i}{m_e}\right)^{1/2} \approx 14 \frac{T_i}{T_e} + 3$$

for hydrogen. With $T_i/T_e = 0.5$, we obtain $v_D/v_i \geq 10$ which has to be compared with $v_D/v_i \sim 6$ for the conditions of Fig. 2(a).

Considering the experimental accuracy (in particular, the radial distribution of v_D is not known), the condition for the critical drift is marginally satisfied at $t = 280$ ms but it is easily fulfilled for $t \leq 100$ ms. For instance, at $t = 20$ ms we have $v_D/v_i \simeq 16$ whereas the critical drift condition yields $v_D/v_i \geq 9$. In Fig. 2(b) we see a threshold at $t = 70$ ms but this result has to be taken at a fixed value of $k_\perp$. Indeed at $t = 50$ ms the condition for maximum growth rate $k_\perp \rho_i \sim 1$ yields $k_\perp = 20$ cm^{-1} which is outside the $k_\perp$ interval $(k_\perp = 11 \pm 3$ cm$^{-1})$.

An order of magnitude of the density fluctuations can be obtained from the absolute calibration of the emitter-receiver system. The dynamic factor

$$S(k_\perp, \omega) = \frac{P_s}{P_{sc}} \frac{\sigma_c}{\sigma_0} \frac{1}{r^4 \Delta f}$$

is obtained by a comparison of the power scattered by the plasma P_s with the power P_{sc} scattered by a metallic sphere positioned in the center of the scattering volume.[6] Here σ_c is the cross section of the metallic sphere, σ_0 is the scattering cross section corrected by the effects of the polarization of the incident wave,[7] r is the linear dimension of the scattering volume, and Δf is the bandwidth of the i.f. amplifier. The total mean-square density fluctuation is given by

$$\langle|\tilde{n}|^2\rangle=(2\pi)^{-3}\int S(\vec{k}_\perp,\omega)\,d^2k_\perp d\omega\simeq 10^{20}\ \mathrm{cm}^{-6},$$

$$(\langle|\tilde{n}|^2\rangle)^{1/2}=0.5\times10^{-3}\bar{n}_e,$$

where we have integrated over the measured frequency spectrum and assumed that the $k_\perp$ spectrum has a maximum at $k_\perp=11\ \mathrm{cm}^{-1}$ and a width $\Delta k=\pm5.5\ \mathrm{cm}^{-1}$. A rough estimate of the amplitude of the current-driven ion-cyclotron turbulence in stationary conditions is given by[8]

$$\eta^2=\frac{\langle|\tilde{n}_e|^2\rangle}{\bar{n}_e^{\,2}}=\frac{1}{\sqrt{2\pi}}\frac{T_e}{T_i}\,\Gamma_1\left(\frac{v_D}{v_e}\right)^5\approx4\times10^{-6},$$

$$(\langle|\tilde{n}|^2\rangle)^{1/2}=2\times10^{-3}\bar{n}_e,$$

which compares well with the measured value.

In the toroidal configuration, the effect of the magnetically trapped electrons has to be considered since in the trapped-electron regime the current-driven instabilities are quenched.[9] For our experimental conditions $\nu_{\mathrm{eff}}/\omega_{be}{}^{(r)}=\nu_e Rq/v_e(2r/R)^{3/2}$, where ν_e is the Coulomb collision frequency of the electrons, R is the major radius, and $q=rB_{\mathrm{tot}}/RB_{\mathrm{pol}}$, has been calculated[10] showing that it is generally larger than unity except in a small region around $r=7$ cm where $\nu_{\mathrm{eff}}/\omega_{be}\approx0.6$. Thus for our experimental conditions, the effect of trapped electrons can be neglected.

For the present experiment, the current-driven mechanism cannot be ruled out, it is expected that for increasing n_e and T_i the critical drift conditions will be hardly fulfilled and for increasing T_e the magnetically trapped electrons should make this instability virtually impossible.

Since $v_D/v_e\sim0.1$, which is lesser than the threshold value 0.3, we also can disregard the effect of a slide-away distribution function.[11]

The presence of a runaway electron tail has been recently proposed to explain the presence of plasma waves $\omega=\omega_{pe}k_\parallel/k$ for a current-carrying magnetized plasma.[12] A mechanism based on a nonlinear coupling between two electron electrostatic waves for generating a wave near Ω_i can be considered and it is now under investigation.

In conclusion, we have presented an experimental observation of density fluctuations in the region of the ion cyclotron frequency. The lack of measurements of the $k_\perp$ spectrum does not permit a quantitative comparison with the theory. However, the qualitative analysis of the results suggests that current-driven instability could explain the present measurements.

[a]J. Adam, J. F. Bonnal, A. Bresson, C. Breton, J. Breton, Ph. Brossier, J. P. Bussac, R. Cano, M. Chatelier, M. Cotsaftis, M. Cranga, J. P. Crenn, R. Dei-Cas, C. De Michelis, J. Druaux, P. Ginot, J. P. Girard, R. Gravier, F. Hennion, J. How, J. Jacquinot, F. Koechlin, H. Kuus, J. Lasalle, D. Launois, P. Lecoustey, J. Lelegard, E. Maschke, M. Mattioli, C. Mercier, P. Moriette, R. Oberson, P. Platz, P. Plinate, G. Ramponi, C. Renaud, A. Samain, S. Schram, N. Siakavellas, Z. Siedziewski, J. L. Soule, J. Tachon, A. Torossian, J. Touche, D. Veron, F. Werkoff, and B. Zanfagna.

[1]R. W. Motley and N. D'Angelo, Phys. Fluids 6, 296 (1963).

[2]W. E. Drummond and M. N. Rosenbluth, Phys. Fluids 5, 1507 (1962).

[3]M. Yamada, H. W. Hendel, S. Seiler, and S. Ichimaru, Phys. Rev. Lett. 34, 650 (1975).

[4]D. R. Dakin, T. Tajima, G. Benford, and N. Rynn, J. Plasma Phys. 15, 175 (1976).

[5]H. W. Hendel and M. Yamada, Phys. Rev. Lett. 33, 1076 (1974).

[6]L. E. Sharp and S. Mrowka, J. Phys. D 8, 2153 (1975).

[7]The scattering cross section for the extraordinary wave has been numerically calculated by E. Mazzucato.

[8]I. Fidone, Plasma Phys. 11, 669 (1969).

[9]V. Arunasalam, M. Okabayashi, R. J. Hawrjluk, and S. Suchewer, Phys. Fluids 20, 95 (1977).

[10]$\nu_{\mathrm{eff}}/\omega_{be}{}^{(r)}$ has been calculated by F. Koechlin.

[11]B. Coppi, F. Pegoraro, R. Pozzoli, and G. Rewoldt, Nucl. Fusion 16, 309 (1976).

[12]K. Molvig, M. S. Tekula, and A. Bers, Phys. Rev. Lett. 38, 1404 (1977).

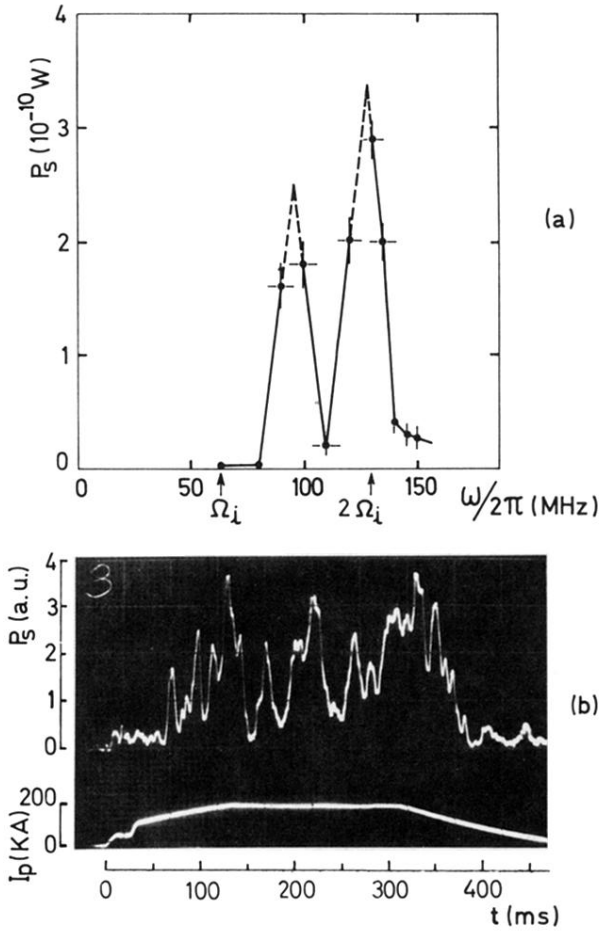

FIG. 2. (a) The scattered power P_s as a function of the frequency $\omega/2\pi$ at $t = 280$ ms. Hydrogen, $\bar{n}_e(r = 11$ cm$) = 1.0 \times 10^{13}$ cm^{-3}, $T_e(r = 11$ cm$) = 800$ eV, $T_e(r = 0) = 2.1$ keV, $I = 200$ kA, $B = 49$ kG, $a = 17$ cm, $T_e/T_i(r = 11$ cm$) = 2$. The arrows indicate the values of Ω_i and $2\Omega_i$ at $r = 11$ cm, the center of the scattering volume. (b) The scattered power P_s as function of time for $\omega/2\pi = 90$ MHz corresponding to the first peak of (a) (upper trace) and the discharge current I (lower trace).